Langmuir
Article
pubs.acs.org/Langmuir

Using Self-Assembled Monolayers to Model Cell Adhesion to the 9th and 10th Type III Domains of Fibronectin†

Jessica L. Eisenberg, Justin L. Piper, and Milan Mrksich*

Department of Chemistry and Howard Hughes Medical Institute, The University of Chicago, Chicago, Illinois 60637

Received April 29, 2009. Revised Manuscript Received July 10, 2009

Most mammalian cells must adhere to the extracellular matrix (ECM) to maintain proper growth and development. Fibronectin is a predominant ECM protein that engages integrin cell receptors through its Arg-Gly-Asp (RGD) and Pro-His-Ser-Arg-Asn (PHSRN) peptide binding sites. To study the roles these motifs play in cell adhesion, proteins derived from the 9th (containing PHSRN) and 10th (containing RGD) type III fibronectin domains were engineered to be in frame with cutinase, a serine esterase that forms a site-specific, covalent adduct with phosphonate ligands. Self-assembled monolayers (SAMs) that present phosphonate ligands against an inert background of tri(ethylene glycol) groups were used as model substrates to immobilize the cutinase-fibronectin fusion proteins. Baby hamster kidney cells attached efficiently to all protein surfaces, but only spread efficiently on protein monolayers containing the RGD peptide. Cells on RGD-containing protein surfaces also displayed defined focal adhesions and organized cytoskeletal structures compared to cells on PHSRN-presenting surfaces. Cell attachment and spreading were shown to be unaffected by the presence of PHSRN when compared to RGD alone on SAMs presenting higher densities of protein, but PHSRN supported an increased efficiency in cell attachment when presented at low protein densities with RGD. Treatment of suspended cells with soluble RGD or PHSRN peptides revealed that both peptides were able to inhibit the attachment of FN10 surfaces. These results support a model wherein PHSRN and RGD bind competitively to integrins—rather than a two-point synergistic interaction—and the presence of PHSRN serves to increase the density of ligand on the substrate and therefore enhance the sticking probability of cells during attachment.

Introduction

The extracellular matrix (ECM) is an insoluble aggregate of fibrous proteins and glycosaminoglycans that serves as the scaffold that organizes the adhesion, growth, and differentiation of mammalian cells.[1−3] In most cases, the integrin receptors—a family of heterodimeric proteins that span the cell membrane—mediate the adhesion of cells to the ECM and transduce both internal and external signals that regulate cellular processes.[4−6] The large number of ligands present in the ECM make it difficult to identify the combinations of ligands and receptors that interact and to understand the downstream activities that result from these interactions.[7,8] Model substrates that present defined binding motifs from ECM proteins have served an important role in addressing this challenge, yet the complications inherent to the immobilization of proteins on culture substrates—including the tendency for proteins to denature and adsorb in nonproductive orientations—can complicate the interpretation of experiments that use model substrates. In this paper, we use self-assembled monolayers (SAMs) that present cell binding domains from fibronectin (FN) as model substrates to address the roles of the FN RGD and PHSRN ligands in cell adhesion.

FN is an ECM protein having a linear arrangement of about thirty domains that includes peptide ligands that mediate the adhesion, spreading, and migration of cells.[9−12] The small peptide Arg-Gly-Asp (RGD) is the prototypical ligand and is located in the 10th type III domain of FN (FN10), where it interacts with several integrin receptors to mediate cell adhesion.[13−15] While this peptide remains the best understood ligand in FN, a substantial effort has addressed the discovery and function of additional ligands that play roles in cell adhesion. Early studies used site-directed mutagenesis and antibody blocking experiments to reveal a motif within the 9th type III domain that also influenced $\alpha5\beta1$ integrin-mediated cell adhesion with baby hamster kidney (BHK) fibroblasts.[16−19] Further mutational studies of this region subsequently identified the specific sequence as Pro-His-Ser-Arg-Asn (PHSRN).[20,21]

† Part of the "Langmuir 25th Year: Self-assembled monolayers: synthesis, characterization, and applications" special issue.

*To whom correspondence should be addressed. E-mail: mmrksich@uchicago.edu.

(1) Beckerle, M. C. *Cell Adhesion*; Oxford University Press: Oxford, 2001.
(2) Alberts, B.; Johnson, A.; Lewis, J.; Raff, M.; Roberts, K.; Walter, P., *Mol. Biol. Cell*, 4th ed.; Garland Science: New York, 2002; pp 1090−1124.
(3) Aukhil, I.; Joshi, P.; Yan, Y.; Erickson, H. P. *J. Biol. Chem.* **1993**, *268*, 2542–2553.
(4) Ginsberg, M. H.; Partridge, A.; Shattil, S. J. *Curr. Opin. Cell Biol.* **2005**, *17*, 509–516.
(5) Arnaout, M. A.; Mahalingam, B.; Xiong, J. P. *Annu. Rev. Cell Dev. Biol.* **2005**, *21*, 381–410.
(6) Luo, B. H.; Carman, C. V.; Springer, T. A. *Annu. Rev. Immunol.* **2007**, *25*, 619–647.
(7) Buck, C. A.; Horwitz, A. F. *Annu. Rev. Cell Biol.* **1987**, *3*, 179–205.
(8) Humphries, J. D.; Byron, A.; Humphries, M. J. *J. Cell Sci.* **2006**, *119*, 3901–3903.
(9) Ruoslahti, E. *Annu. Rev. Biochem.* **1988**, *57*, 375–413.
(10) Pierschbacher, M. D.; Hayman, E. G.; Ruoslahti, E. *J. Cell Biochem.* **1985**, *28*, 115–126.
(11) Aota, S.; Nagai, T.; Olden, K.; Akiyama, S. K.; Yamada, K. M. *Biochem. Soc. Trans.* **1991**, *19*, 830–835.
(12) Ruoslahti, E. *Annu. Rev. Cell Dev. Biol.* **1996**, *12*, 697–715.
(13) Pierschbacher, M. D.; Ruoslahti, E. *Nature* **1984**, *309*, 30–33.
(14) Ruoslahti, E.; Pierschbacher, M. D. *Cell* **1986**, *44*, 517–518.
(15) Ruoslahti, E.; Pierschbacher, M. D. *Science* **1987**, *238*, 491–497.
(16) Obara, M.; Kang, M. S.; Yamada, K. M. *Cell* **1988**, *53*, 649–657.
(17) Kimizuka, F.; Ohdate, Y.; Kawase, Y.; Shimojo, T.; Taguchi, Y.; Hashino, K.; Goto, S.; Hashi, H.; Kato, I.; Sekiguchi, K.; et al. *J. Biol. Chem.* **1991**, *266*, 3045–3051.
(18) Nagai, T.; Yamakawa, N.; Aota, S.; Yamada, S. S.; Akiyama, S. K.; Olden, K.; Yamada, K. M. *J. Cell Biol.* **1991**, *114*, 1295–1305.
(19) Aota, S.; Nagai, T.; Yamada, K. M. *J. Biol. Chem.* **1991**, *266*, 15938–15943.
(20) Bowditch, R. D.; Hariharan, M.; Tominna, E. F.; Smith, J. W.; Yamada, K. M.; Getzoff, E. D.; Ginsberg, M. H. *J. Biol. Chem.* **1994**, *269*, 10856–10863.
(21) Aota, S.; Nomizu, M.; Yamada, K. M. *J. Biol. Chem.* **1994**, *269*, 24756–24761.

Adhesion studies of HT-1080 and BHK-21 cells to surfaces that were modified by the adsorption of recombinant fragments of FN led to the suggestion that the PHSRN peptide was a synergy ligand in $\alpha5\beta1$ integrin-mediated adhesion, since cells were observed to attach and spread to a greater degree on surfaces that presented both the 9th and 10th domains relative to those that presented the 10th domain alone, but cells did not attach to surfaces that lacked the RGD sequence.[17,21−23] Several experiments suggested that the relative spacing of the PHSRN and RGD peptides within FN were important to this synergistic activity, including poor adhesion to proteins having altered linkers between the 9th and 10th domains,[17,24] molecular models,[20,21] and X-ray crystallographic structures of the FN7−10 domains[25] as well as the extracellular region of integrin $\alpha V\beta3$.[26] These studies led to the suggestion that the RGD and PHSRN peptides could interact with different faces of a single $\alpha5\beta1$ integrin, leading to an increased affinity of the receptor when both peptide ligands were present. In this model, the PHSRN peptide presumably has an affinity that is insufficient to mediate adhesion on its own, a feature that is supported by BHK cell adhesion experiments.[22,24] Several studies reported results that are consistent with the synergistic binding model.[27−31]

Other work, however, has found that the RGD and PHSRN ligands bind competitively to the integrin receptor, either by interacting with overlapping regions of the integrin receptor or with nonoverlapping sites that are allosterically connected. In a previous study, we used SAMs that presented the two peptides against an otherwise inert background to find that BHK-21 and NIH-3T3 fibroblast cells use the $\alpha5\beta1$ integrin to attach to surfaces presenting the PHSRN peptide alone, and that this attachment could be blocked by either soluble RGD or PHSRN.[32] That study also showed that PHSRN has a lower affinity for the integrin receptor than does the RGD peptide, consistent with the poor spreading of adherent cells on the former. Other reports have supported the finding that PHSRN alone is able to mediate 3T3 fibroblast and PC12 pheocytochroma cell attachment.[33,34] In addition, a previous study investigated $\beta1$-mediated adhesion and observed PAC1 cell attachment and spreading on several surfaces coated with various recombinant FN type III domains lacking the RGD sequence as long as the integrins had been externally activated,[35] thereby showing that $\beta1$ integrin-mediated cell attachment may not require the RGD motif. The competitive binding of the PHSRN and RGD ligands to the integrin receptor has also been demonstrated for $\alpha IIb\beta3$ integrins, where both PHSRN and RGD peptides were shown to inhibit the binding of the integrin with FN.[20] That study also found that the PHSRN peptide had a lower binding affinity for the integrin than did the RGD peptide, in agreement with our report that used monolayers as model substrates. Collectively, this body of work establishes that the PHSRN motif plays a role in mediating cell adhesion and suggests a revision of the mechanism by which PHSRN and RGD cooperate in adhesion.

The conflicting results summarized above stem in part from the different approaches used to mimic the ECM. The most common approaches rely on the adsorption of recombinant or purified proteins to glass or plastic cultureware and have the primary limitation that the activities of the adsorbed proteins are difficult to determine or to control. Because proteins adsorb with a range of orientations and undergo denaturation to various degrees, the fraction of protein that presents ligand in a state that can interact with cell-surface receptors is often unknown. Studies frequently make the assumption that surfaces presenting proteins that are substantially the same will adsorb in a similar manner to give a constant activity. Yet, several studies have shown that even a single site mutation can dramatically affect the adsorption of proteins. Two cytochrome 5 proteins that only differed in the swapping of two residues were found to adsorb with kinetics that differed by 20-fold.[36] It is also the case that the choice of material can have a dramatic effect on the activity of an adsorbed protein. One study compared three different polystyrene surfaces that were coated with FN and found that C2C12 myoblast cells displayed differences in growth and differentiation simply because, upon adsorption, the FN was not presented in the same manner for each substrate.[37] Another study found that positively charged, negatively charged, or neutral surfaces that were subsequently coated with FN resulted in cells with distinct differences in focal adhesion distributions, signaling activities, and osteoblast differentiation rates.[38]

These challenges with protein-coated substrates have led many groups to employ peptide-modified substrates, where orientation and structure of the active ligands can be controlled better.[39−42] Even here though, nonspecific adsorption of protein to the surface can alter the ligands that are presented to a cell, and the microenvironment around peptides can strongly affect cell adhesion.[43−45] It is the affinities of the immobilized peptides that are differentially impacted by adsorption, and there is the risk that adsorption leads to a loss of affinity of the immobilized peptide. There is also the view that protein-modified substrates have a higher relevance to the ECM than do peptide-modified substrates and are therefore preferred.[46−48]

The present work uses SAM substrates to present recombinant protein domains from FN to study the roles of the PHSRN and RGD motifs in mediating cell adhesion. These substrates are effective models of the ECM because they present protein

(22) Mardon, H. J.; Grant, K. E. *FEBS Lett*. **1994**, *340*, 197–201.
(23) Obara, M.; Yoshizato, K. *Exp. Cell Res*. **1995**, *216*, 273–276.
(24) Grant, R. P.; Spitzfaden, C.; Altroff, H.; Campbell, I. D.; Mardon, H. J. *J. Biol. Chem*. **1997**, *272*, 6159–6166.
(25) Leahy, D. J.; Aukhil, I.; Erickson, H. P. *Cell* **1996**, *84*, 155–164.
(26) Xiong, J. P.; Stehle, T.; Diefenbach, B.; Zhang, R.; Dunker, R.; Scott, D. L.; Joachimiak, A.; Goodman, S. L.; Arnaout, M. A. *Science* **2001**, *294*, 339–345.
(27) Mould, A. P.; Askari, J. A.; Aota, S.; Yamada, K. M.; Irie, A.; Takada, Y.; Mardon, H. J.; Humphries, M. J. *J. Biol. Chem*. **1997**, *272*, 17283–17292.
(28) Burrows, L.; Clark, K.; Mould, A. P.; Humphries, M. J. *Biochem. J*. **1999**, *344* Pt 2, 527-533.
(29) Danen, E. H.; Aota, S.; van Kraats, A. A.; Yamada, K. M.; Ruiter, D. J.; van Muijen, G. N. *J. Biol. Chem*. **1995**, *270*, 21612–21618.
(30) van der Walle, C. F.; Altroff, H.; Mardon, H. J. *Protein Eng*. **2002**, *15*, 1021–1024.
(31) Altroff, H.; van der Walle, C. F.; Asselin, J.; Fairless, R.; Campbell, I. D.; Mardon, H. J. *J. Biol. Chem*. **2001**, *276*, 38885–38892.
(32) Feng, Y.; Mrksich, M. *Biochemistry* **2004**, *43*, 15811–15821.
(33) Dankers, P. Y.; Harmsen, M. C.; Brouwer, L. A.; van Luyn, M. J.; Meijer, E. W. *Nat. Mater*. **2005**, *4*, 568–574.
(34) Cooke, M. J.; Phillips, S. R.; Shah, D. S. H.; Athey, D.; Lakey, J. H.; Przyborski, S. A. *Cytotechnology* **2008**, *56*, 71–79.
(35) Chi-Rosso, G.; Gotwals, P. J.; Yang, J.; Ling, L.; Jiang, K.; Chao, B.; Baker, D. P.; Burkly, L. C.; Fawell, S. E.; Koteliansky, V. E. *J. Biol. Chem*. **1997**, *272*, 31447–31452.
(36) Ramsden, J. J.; Roush, D. J.; Gill, D. S.; Kurrat, R.; Willson, R. C. *J. Am. Chem. Soc*. **1995**, *117*, 8511–8516.
(37) Garcia, A. J.; Vega, M. D.; Boettiger, D. *Mol. Biol. Cell* **1999**, *10*, 785–798.
(38) Keselowsky, B. G.; Collard, D. M.; Garcia, A. J. *Biomaterials* **2004**, *25*, 5947–5954.
(39) Massia, S. P.; Hubbell, J. A. *J. Cell Biol*. **1991**, *114*, 1089–1100.
(40) Mardilovich, A.; Kokkoli, E. *Biomacromolecules* **2004**, *5*, 950–957.
(41) Mardilovich, A.; Craig, J. A.; McCammon, M. Q.; Garg, A.; Kokkoli, E. *Langmuir* **2006**, *22*, 3259–3264.
(42) Benoit, D. S.; Anseth, K. S. *Biomaterials* **2005**, *26*, 5209–5220.
(43) Houseman, B. T.; Mrksich, M. *Biomaterials* **2001**, *22*, 943–955.
(44) Ochsenhirt, S. E.; Kokkoli, E.; McCarthy, J. B.; Tirrell, M. *Biomaterials* **2006**, *27*, 3863–3874.
(45) Takagi, J. *Biochem. Soc. Trans*. **2004**, *32*, 403–406.
(46) Petrie, T. A.; Capadona, J. R.; Reyes, C. D.; Garcia, A. J. *Biomaterials* **2006**, *27*, 5459–5470.
(47) Richman, G. P.; Tirrell, D. A.; Asthagiri, A. R. *J. Controlled Release* **2005**, *101*, 3–12.
(48) Cutler, S. M.; Garcia, A. J. *Biomaterials* **2003**, *24*, 1759–1770.

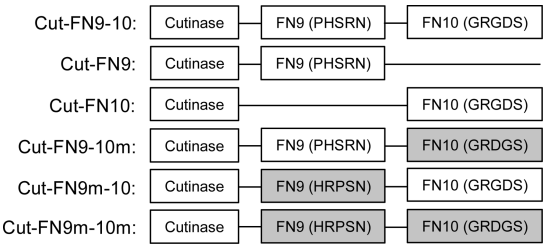

Figure 1. Constructs of the FN type III domains fused to the C-terminal end of cutinase, where the mutated integrin-binding peptide sites of the domains are indicated in gray.

domains in a homogeneous microenvironment and with control over density and orientation. Additionally, monolayers that present the tri(ethylene glycol) group resist the nonspecific adsorption of protein and maintain defined interactions between the cell and the substrate. We show that BHK fibroblast cells adhere to substrates that present PHSRN but lack RGD, consistent with an earlier study in which peptide substrates were used.[32] Interestingly, we initially did not observe a higher level of cell attachment to surfaces presenting both ligands. For substrates presenting lower densities of protein, however, we find that the presence of PHSRN with RGD leads to more efficient cell adhesion compared to substrates presenting RGD alone. We also show that both soluble PHSRN and RGD peptides are able to inhibit cell adhesion to substrates presenting FN10, indicating that the two peptide ligands bind competitively to the same site of the integrin receptor. The use of well-defined protein substrates in this work supports a model where PHSRN and RGD act as individual, competitive ligands to mediate cell adhesion.

Experimental Methods

Protein Construction and Expression. The construction of the vector containing the cutinase gene, pCut22b, was described elsewhere.[49] The plasmid FNIII7−10(pET11b), containing the 7th, 8th, 9th, and 10th type III repeat domains of FN, was provided by Dr. Harold Erickson (Duke University, Durham, NC).[25] Details on the gene splicing by overlap extension polymerase chain reaction (SOEing PCR) technique and the primers used to make the Cut-FN domain fusions can be found in the Supporting Information. Separate constructs were prepared for expression of Cut-FN9−10, Cut-FN9, Cut-FN10, Cut-FN9−10m (where the RGD site was scrambled to RDG), Cut-FN9m−10 (where the PHSRN site was scrambled to HRPSN), and Cut-FN9m−10m (the double mutant form) shown in Figure 1. All products were verified through DNA sequencing.

Cultures of BL21(DE3) cells (Invitrogen, Carlsbad, CA) containing the plasmids for each Cut-FN protein were grown at 37 °C to an OD_{600} of 0.5. Expression was then induced with 0.5 mM isopropyl β-D-1-thiogalactopyranoside (IPTG; Sigma, St. Louis, MO). All the proteins except Cut-FN9 were expressed for 16−18 h at 22 °C. Cut-FN9 was expressed at 15 °C for 16−18 h to increase the yield of the soluble protein. The cell pellets were lysed via sonication into phosphate-buffered saline (PBS) containing 1× complete protease inhibitors (Roche, Indianapolis, IN). The lysates were clarified through centrifugation and stored at 4 °C for up to one month. Protein expression levels were determined by a cutinase activity assay as described previously.[49]

Preparation of SAM Substrates. Monolayer substrates were prepared as described previously.[49,50] Briefly, titanium (40 Å) then gold (220 Å) were evaporated onto glass coverslips using an electron beam evaporator (Thermionics) at a rate of 0.2−0.4 nm/s at a pressure of 1.0×10^{-6} Torr. Monolayers were formed by immersing these substrates into an ethanolic solution containing a mixture of a symmetric tri(ethylene glycol)-terminated disulfide (EG_3) and an asymmetric disulfide with tri(ethylene glycol) and maleimide head groups for 12−16 h at room temperature. The disulfide reagents were used at a concentration of 0.5 mM with the maleimide-terminated reagent present at relative fractions of 5% to 0.001%. All substrates were washed with ethanol and dried with a stream of nitrogen.

The phosphonate ligand was synthesized by modifying a previously described method[49] and was dissolved in a 1:1 mixture of PBS and ethanol at 0.01 mg/mL and applied to maleimide-terminated monolayers for 2 h at room temperature (Figure 2A). For the preparation of monolayers having very low densities of phosphonate, the reagent was diluted with 6-mercapto-1-hexanol (Sigma) in various molar ratios to decrease the phosphonate ligand immobilized on the surface. In all cases, the surfaces were rinsed with water and ethanol and dried under a stream of nitrogen prior to use. The phosphonate-presenting SAMs were immersed in crude bacterial lysates containing the recombinantly expressed cutinase−fibronectin domain fusion proteins for 2 h to covalently immobilize the desired protein to the SAMs. The monolayers were then rinsed with 0.5% sodium dodecyl sulfate (SDS) to remove noncovalently immobilized proteins,[49,51] followed by PBS before use in cell adhesion experiments. Figure 2B displays the schematic for Cut-FN domain immobilization, while Figure 2C shows the SAMDI spectra that verifies immobilization of the ligands.

Positive control surfaces were prepared by immersing the bare gold surfaces in a 1 mM ethanolic solution of dodecanethiol overnight. The surfaces were then rinsed with ethanol and dried under nitrogen. Full-length human FN (Sigma), at 25 μg/mL in PBS, was applied to the monolayers for 2 h at room temperature. These substrates were rinsed with PBS. Negative control surfaces consisted of either EG_3 monolayers that had formed overnight and incubated with bacterial lysates containing the Cut-FN domain proteins or phosphonate SAMs to which recombinantly expressed cutinase was immobilized. In both of these cases, the chips were rinsed with 0.5% SDS and PBS.

Matrix-Assisted Laser Desorption/Ionization Mass Spectrometry of SAMs (SAMDI). Following each step used to prepare the substrates described above, the samples were characterized by SAMDI mass spectrometry. Spectra were obtained using a 4800 MALDI-TOF/TOF mass spectrometer (Applied Biosystems, Framingham, MA) using 2′,4′,6′-trihydroxyacetophenone (10 mg/mL) in acetonitrile as the matrix for the lower molecular weight substrates and α-cyano-4-hydroxycinnamic acid (7.5 mg/mL) in acetone for the immobilized protein substrates.

Cell Culture. BHK-21 cells (ATCC, Rockville, MD) were cultured in low-glucose Dulbecco's modified Eagle medium (DMEM; GIBCO, Carlsbad, CA) supplemented with 2 mM L-glutamine (GIBCO). NIH-3T3 cells (ATCC) were cultured in high-glucose DMEM supplemented with 4 mM L-glutamine. In both cases, the media were also supplemented with 10% fetal bovine serum and 1× penicillin/streptomycin (GIBCO). Cells were cultured at 37 °C with 5% CO_2.

Cell Adhesion Assays. Confluent monolayers of BHK or 3T3 cells were removed from culture flasks and counted. Thirty thousand cells were added to monolayers measuring 1 cm^2 in size and incubated on the monolayers for 1 h at 37 °C with 5% CO_2 before the chips were rinsed with fresh media. Live cell images were captured using a charge-coupled device (CCD) camera attached to an Axiovert 200 microscope from Zeiss and Openlab software (Improvision, Lexington, MA). The cells were then fixed

(49) Hodneland, C. D.; Lee, Y. S.; Min, D. H.; Mrksich, M. *Proc. Natl. Acad. Sci. U.S.A.* **2002**, *99*, 5048–5052.
(50) Houseman, B. T.; Gawalt, E. S.; Mrksich, M. *Langmuir* **2003**, *19*, 1522–1531.
(51) Murphy, W. L.; Mercurius, K. O.; Koide, S.; Mrksich, M. *Langmuir* **2004**, *20*, 1026–1030.

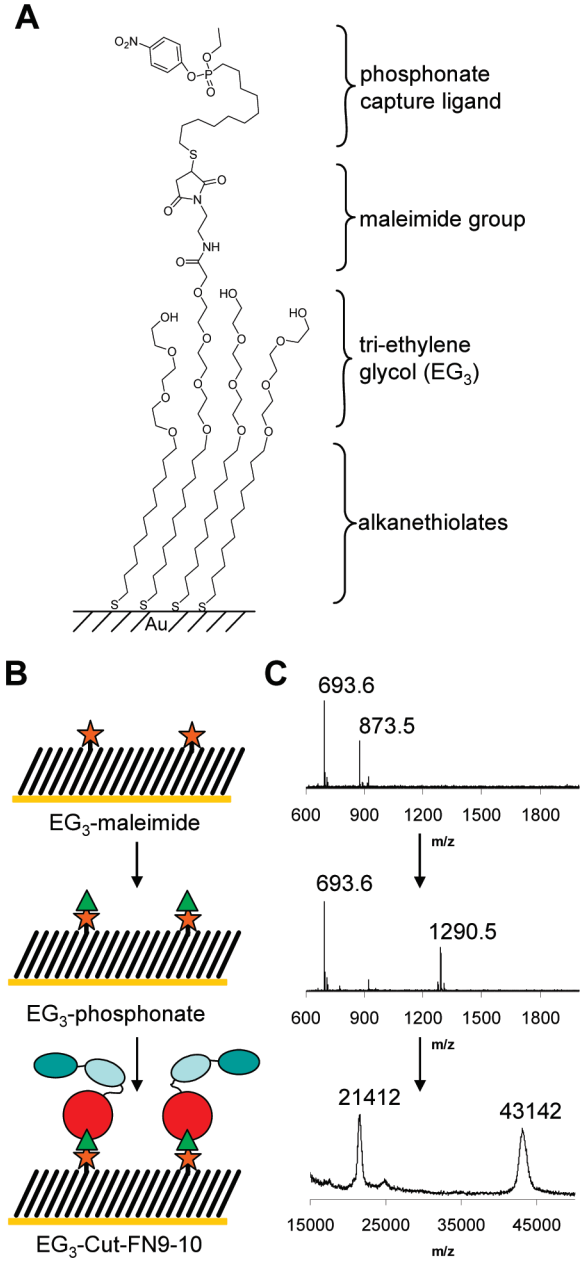

Figure 2. (A) SAMs presenting a phosphonate capture ligand for the covalent immobilization of cutinase−fibronectin fusion proteins. (B) Substrates were prepared by first treating a maleimide-terminated monolayer with a phosphonate ligand and then with a cutinase fusion protein to immobilize the FN fragments. (C) SAMDI mass spectrometry was used to confirm the masses of the ligands presented on the surface after each step.

using 3.7% formaldehyde in PBS, and 4′,6-diamidino-2-phenylindole (DAPI; Molecular Probes, Eugene, OR) and Alexa 488-labeled phalloidin (Molecular Probes) were added at dilutions of 1:10 000 and 1:1000 to stain the nuclei and actin filaments, respectively. After rinsing, the substrates were fluorescently imaged on the Axiovert 200. Images of the nuclei were captured in five places for each chip through a 20× objective (660 μm by 500 μm field of view) and counted using a nucleus counter plug-in for ImageJ (NIH). The total area of fluorescence for each field was obtained by thresholding the actin images and calculating the total fluorescent area using ImageJ. The total area of fluorescence was then divided by the total number of nuclei within the same fields to yield the average cell area. Each type of cell adhesion experiment was repeated in triplicate, and five images were captured per chip to ensure the reproducibility of the results. Statistical analysis was done following the Student's t test.

Immunostaining. BHK cells were added to each substrate for 4 h with complete media to attach and spread. Substrates were washed with PBS prior to fixation with 3.7% formaldehyde for 5 min, followed by 1 min of permeabilization with 0.3% Triton X-100 in PBS and 1 h with blocking buffer (1% bovine serum albumin (BSA), 5% goat serum, and 0.1% Triton X-100). Substrates were then incubated with a mouse antihuman vinculin (Sigma) primary antibody at 1:1000 in blocking buffer for 1 h, followed by a goat antimouse IgG antibody labeled with Texas Red (Molecular Probes) at a 1:1000 dilution, Alexa 488-labeled phalloidin, and DAPI. All substrates were rinsed thoroughly with blocking buffer and mounted with 80% glycerol. Fluorescent images were captured using an Axiovert 200 with Openlab software and a 100× objective.

Inhibition Assay. Suspensions of 50 000 BHK cells in serum-free media were incubated with soluble cyclic-RGDfC, GRGDS, PHSRN, GRDGS, or HRPSN peptide inhibitors at concentrations ranging from 5 μM to 1 mM for 15 min at room temperature. The linear peptides were synthesized using standard Fmoc solid-phase synthesis (reagents from AnaSpec, San Jose, CA), and the cyclic peptide was made as previously described.[52] The cell−peptide solutions were added to SAMs presenting either 0.005% FN10 (for RGD inhibitions) or 0.001% FN10 (for PHSRN inhibitions) and incubated for an additional 15 min at 37 °C. The chips were then transferred to a clean well plate, rinsed with PBS, and fixed with 3.7% formaldehyde in PBS. The nuclei of the fixed cells were stained with DAPI and counted in eight different places for each substrate in three independent experiments. The average level of cell attachment inhibition was reported with respect to the control surfaces that included no peptide inhibitors.

Results

Monolayer Substrates Presenting FN Domains. We designed several cutinase−fibronectin fusion proteins to investigate the roles of PHSRN and RGD in cell adhesion. We used the two domains from FN that carry the RGD and PHSRN ligands to prepare three native proteins (FN9−10, FN9, and FN10). We also engineered three mutated proteins wherein the PHSRN sequence was scrambled (HRPSN; FN9m−10), the RGD sequence was scrambled (RDG; FN9−10m), and where both peptides were scrambled (FN9m−10m). These domains were expressed as fusion proteins with cutinase and immobilized to monolayers presenting phosphonate. The phosphonate group is an irreversible ligand for cutinase and is used to covalently tether proteins in a defined orientation to the monolayer.[49,51,53] This feature, along with the EG_3 groups that prevent the nonspecific adsorption of protein,[54−56] allowed us to selectively immobilize the constructs using crude bacterial lysates and without the need for prior purification.

Extensive work has shown that SAMs are compatible with matrix-assisted laser desorption/ionization mass spectrometry, which allows for straightforward characterization of the ligands

(52) Kato, M.; Mrksich, M. *Biochemistry* **2004**, *43*, 2699–2707.
(53) Kwon, Y.; Han, Z.; Karatan, E.; Mrksich, M.; Kay, B. K. *Anal. Chem.* **2004**, *76*, 5713–5720.
(54) Mrksich, M. *Curr. Opin. Chem. Biol.* **2002**, *6*, 794–797.
(55) Ostuni, E.; Yan, L.; Whitesides, G. M. *Colloids Surf. B: Biointerfaces* **1999**, *15*, 3–30.
(56) Mrksich, M.; Whitesides, G. M. Using self-assembled monolayers that present oligo(ethylene glycol) groups to control the interactions of proteins with surfaces. In *American Chemical Society Symposium Series on Chemistry and Biological Applications of Polyethylene Glycol*,; American Chemical Society: Washington, DC, 1997; Vol. *680*, pp 361−373.

presented on the surfaces.[57−61] We have termed this characterization technique SAMDI and used this method to confirm the immobilization of each Cut-FN domain protein to the monolayer substrates in this work (Figure 3). The resulting spectra display peaks corresponding to the desired proteins as both the double- and single-charged species, as has been seen previously with SAMDI spectra of proteins.[59,60] Cut-FN9 and Cut-FN10 have predicted molecular weights of 33 kDa, while Cut-FN9−10, Cut-FN9−10m, Cut-FN9m−10, and Cut-FN9m−10m have expected molecular weights of 43 kDa.

Cell Adhesion to the Monolayer Substrates. We first verified that BHK cells would attach and spread on the FN9−10 substrates with similar morphology as they do on the FN-coated substrates typically used in adhesion studies. We seeded the cells onto surfaces with adsorbed full length FN (Figure 4A) and compared the levels of cell attachment onto FN9−10 surfaces at 1% ligand density (Figure 4B). We observed that similar numbers of cells attached to both surfaces, and in both cases had cells that were well-spread within the first hour of culture and exhibited the typical fibroblast cell morphology. We then assessed adhesion on the remaining five engineered protein substrates. The number of cells that attached to FN9, FN10, FN9−10m, and FN9m−10 (Figure 4 C−F) was similar to that for FN9−10. However, cells on FN9 and FN9−10m surfaces were smaller and exhibited round morphologies compared to cells on the FN9−10, FN10, and FN9m−10 substrates. This difference was expected since the PHSRN peptide ligand has been shown to have a lower affinity for integrin receptors and sustain only rounded cells.[32] We observed no significant adhesion to surfaces displaying the double mutant protein FN9m−10m (Figure 4G), which confirms that the adhesion is specific to the PHSRN and RGD peptide ligands. There was also no adhesion to other control surfaces that presented either EG_3 groups with no protein domains (Figure 4H) or immobilized cutinase (Figure 4I), again indicating the observed cell adhesion was specific for the FN protein domains. We also performed the adhesion experiments using 3T3 cells and saw similar results (data not shown). These results are consistent with a previous study showing that BHK and 3T3 cells attached to peptide surfaces presenting either PHSRN or RGD.[32]

To quantify the number of cells attached and spread on each surface, BHK cells (30 000 cells) were applied to monolayers for 1 h, then fixed and stained for nuclei and actin. Several images were collected with a 20× objective, and the number of cells was averaged for each substrate as described in the Experimental Methods section (Figure 5). Each of the substrates had about 20 adherent cells per imaging frame, except the double mutant FN9m−10m, which had less than 5 cells. The cells adherent to substrates presenting the RGD motif had an average cell area of approximately 900 μm^2, whereas cells on substrates having the PHSRN motif, but lacking the RGD motif, had an average cell area of approximately 250 μm^2. The few cells that had attached to the control surfaces devoid of adhesive ligand also averaged 250 μm^2 in size, leading us to designate a cell as spread if its area was above this minimum value. For the monolayers presenting FN9 and FN9−10m, only about 20% of the cells had areas above 250 μm^2 and were designated as spread; however, these cells maintained round morphologies due to the decreased affinity to the substrates lacking the RGD motif. In contrast, more than 70% of cells on monolayers presenting FN, FN9−10, FN10, and FN9m−10 (proteins with RGD) had cell areas above 250 μm^2, and these cells exhibited typical fibroblast morphologies. Also interesting, when comparing cells on FN9−10 to those on FN10 and FN9m−10, we failed to observe

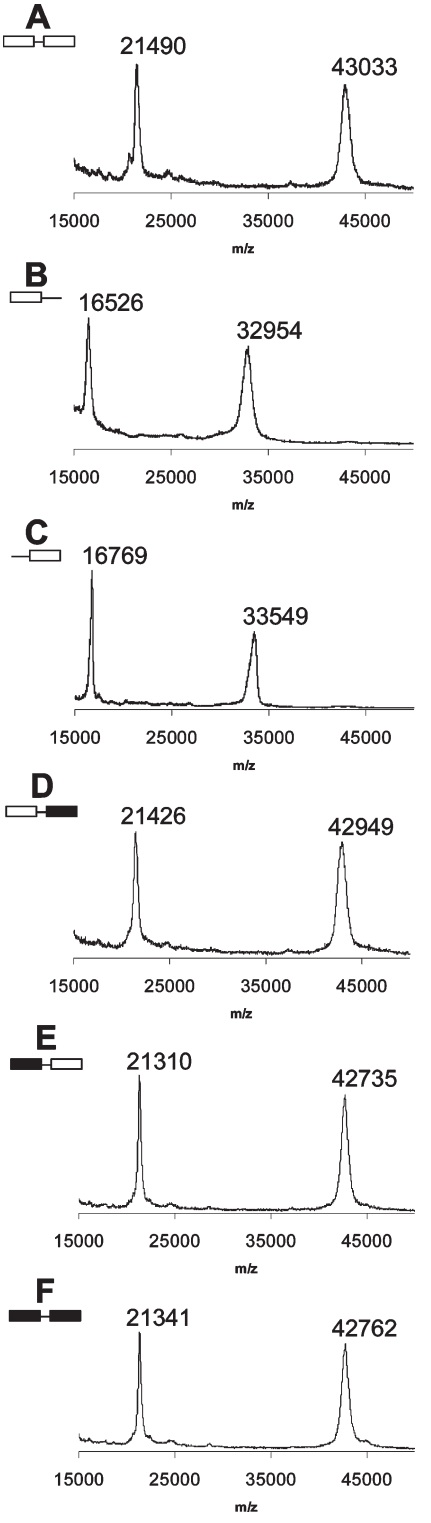

Figure 3. The expression and immobilization of the six Cut-FN proteins was confirmed with SAMDI mass spectrometry. The spectra show the expected products as the double- and single-charged species. The domains constructed with mutated integrin-binding peptide sequences are indicated in gray. (A) Cut-FN9−10, (B) Cut-FN9, (C) Cut-FN10, (D) Cut-FN9−10m, (E) Cut-FN9m−10, and (F) Cut-FN9m−10m.

(57) Su, J.; Mrksich, M. *Angew. Chem., Int. Ed. Engl.* **2002**, *41*, 4715–4718.
(58) Yeo, W. S.; Min, D. H.; Hsieh, R. W.; Greene, G. L.; Mrksich, M. *Angew. Chem., Int. Ed. Engl.* **2005**, *44*, 5480–5483.
(59) Patrie, S. M.; Mrksich, M. *Anal. Chem.* **2007**, *79*, 5878–5887.
(60) Marin, V. L.; Bayburt, T. H.; Sligar, S. G.; Mrksich, M. *Angew. Chem., Int. Ed. Engl.* **2007**, *46*, 8796–8798.
(61) Mrksich, M. *ACS Nano* **2008**, *2*, 7–18.

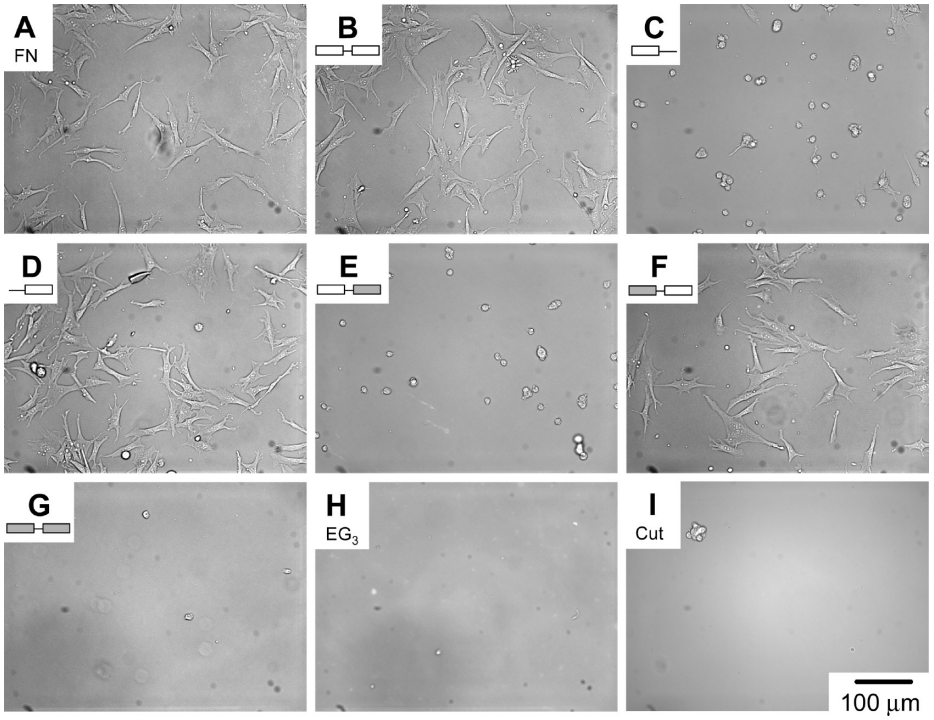

Figure 4. Optical micrographs of BHK cells adherent to monolayers presenting (A) adsorbed, full length FN, (B) FN9−10, (C) FN9, (D) FN10, (E) FN9−10m, and (F) FN9m−10, but not to (G) FN9m−10m. Cells also did not attach to control surfaces presenting either (H) EG_3 or (I) cutinase.

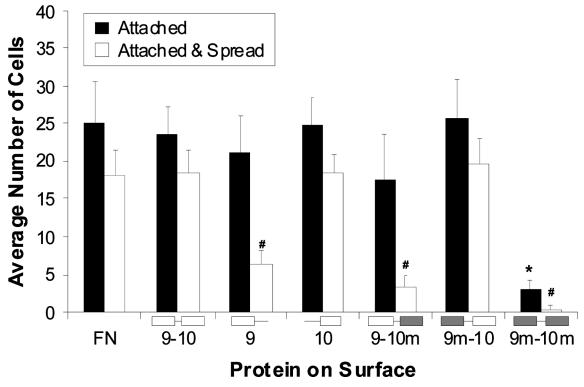

Figure 5. Number of BHK cells attached and spread on protein surfaces. The average number of attached cells per field of view through a 20× objective is shown in black, and the average number of these cells that are spread above 250 μm^2 is indicated in white. The data reveal a similar level of cell attachment to each of the protein surfaces (except FN9m−10m), but few cells attached to substrates lacking RGD were spread. The experiment was performed in triplicate, and average values were determined from images captured in five locations per chip. The asterisk indicates that attachment to FN9m−10m was statistically significant from attachment to the other substrates with $p < 0.0005$, and the pound symbol indicates the number of spread cells on FN9, Fn9−10m, and FN9m−10m was significantly less than the that on the other substrates with $p < 0.0005$.

a dependence of adhesion, spreading, or morphology due to the presence of the PHSRN motif.

In a separate experiment, we allowed cells to adhere for four hours to each of the monolayer substrates and then fixed and immunostained the samples to compare the development of focal adhesions (FAs) and the cytoskeleton (Figure 6). We observed that cells spread well on the FN, FN9−10, FN10, and FN9m−10 surfaces, and these cells also displayed abundant vinculin-containing FA structures and organized actin cytoskeletons spanning the entire cells. In contrast, we found almost no localization of vinculin and a lack of organized actin structures in cells attached to FN9 and FN9−10m. We found a similar trend in experiments that used 3T3 cells (data not shown).

Dependence of Cell Attachment and Spreading on Density of Adhesion Ligand. Because we failed to observe a role for the PHSRN motif in promoting attachment or spreading of cells to monolayers presenting the RGD motif—as has been observed in other studies that led to the proposal of the synergistic binding model—we questioned whether the density of the RGD motif in our substrates might be high enough to mask the role of the lower affinity PHSRN motif. Monolayers presenting ligand at high density—relative, for example, to the density of integrin receptor on the cell surface—might mask the effect of the synergy ligand in cell adhesion; therefore we compared cell adhesion to a series of monolayers where the density of ligand was decreased. Adhesion experiments using substrates presenting FN9 and FN9−10m at lower densities, however, showed a considerable reduction in the number of attached cells (see Supporting Information Figure S1), likely due to the lower affinity of this ligand for the integrin, as has been previously reported.[32] We proceeded with monolayers presenting the maleimide group at a density of 0.1% relative to total alkanethiolate and treated these surfaces with mixtures of the phosphonate reagent and 6-mercapto-1-hexanol (which serves to dilute the former on the monolayer) and then treated each of these monolayers with the protein constructs. In this way we prepared a series of monolayers having a relative density of protein that spans a range of 10^4—including surfaces where all of the maleimide was conjugated to 6-mercapto-1-hexanol and therefore unable to specifically immobilize the FN proteins—in order to determine whether a synergy effect would be observed at a lower ligand density.

As described above, we determined the average number of cells that attached to monolayers presenting FN9−10, FN10, and FN9m−10 for each density of protein (Figure 7A). Cells attached

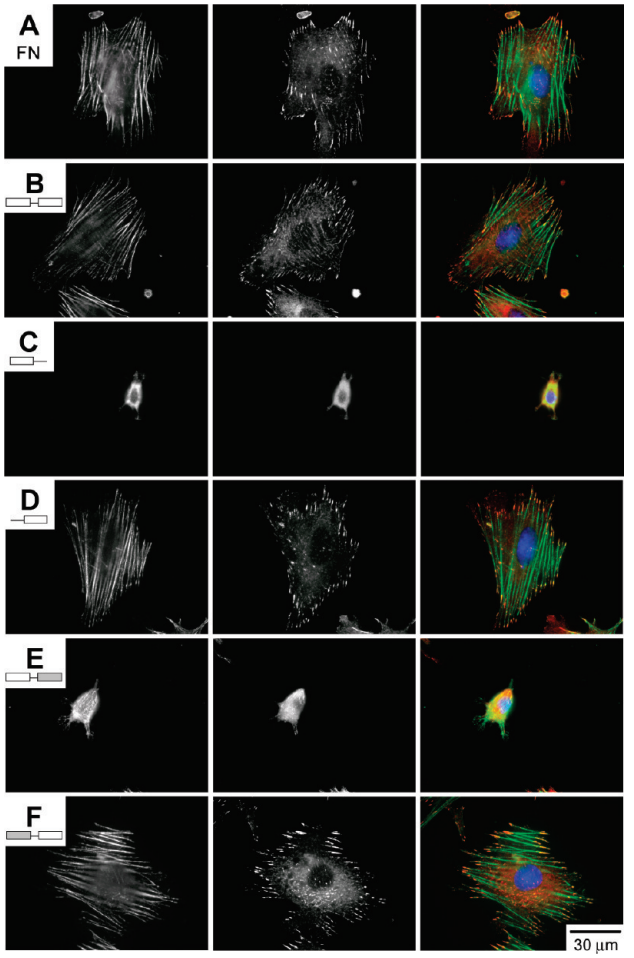

Figure 6. Representative BHK cells attached to (A) adsorbed, full length FN, (B) FN9−10, (C) FN9, (D) FN10, (E) FN9−10m, and (F) FN9m−10 and were fixed and stained for actin (left) and vinculin (middle). The overlay images on the right show the cytoskeleton in green, FAs in red, and nuclei in blue. Cells on surfaces lacking the RGD sequence (C,E) remain poorly spread and display less-defined cytoskeletons and FAs than those presenting RGD (A,B,D,F).

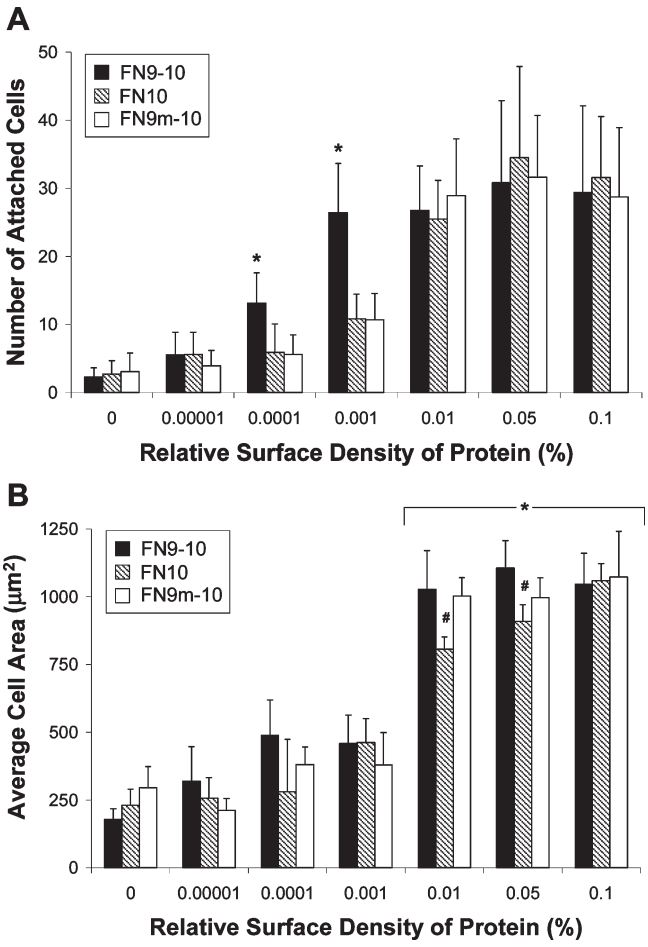

Figure 7. Cell attachment and spreading were quantified for substrates presenting FN9−10, FN10, and FN9m−10 at densities ranging from 0.00001 to 0.1%. (A) Cells adhered to substrates presenting FN9−10 at densities down to 0.0001% protein, while no attachment to FN10 and FN9m−10 was observed below a density of 0.001%. The average number of cells that attached to substrates presenting FN9−10 substrates at densities of 0.001% and 0.0001% were statistically greater than the averages for FN10 and FN9m−10 at the same densities (asterisk indicates $p < 0.0005$). (B) Cell spreading significantly increased for all three proteins above a density of 0.01% protein. Cells on FN10 remained slightly less spread than FN9−10 and FN9m−10 for surfaces presenting protein at densities of 0.05% and 0.01% (asterisk indicates $p < 0.0005$; pound symbol indicates $p < 0.025$). Averages were determined from three experiments, where seven images were captured per chip.

comparably to surfaces having densities of protein ranging from 0.01 to 0.1%, with approximately 20 cells attached per field of view. For surfaces lacking the PHSRN ligand, attachment dropped to 5−10 cells per field at densities ranging from 0.0001 to 0.001%. These levels of cell attachment were significantly lower than those observed to FN9−10 surfaces, where the average number of attached cells remained at 13 cells and 26 cells per field at 0.0001% and 0.001% densities, respectively. This significant decrease in adhesion to FN10 and FN9m−10 reveals that the presence of PHSRN has a measurable effect on cell attachment at lower densities. Additionally, there was no cell adhesion to substrates where the maleimide was conjugated to 6-mercapto-1-hexanol and then incubated with the FN protein lysates (labeled 0% relative surface density of protein), indicating these surfaces remained inert to nonspecific protein adsorption.

We also determined the average projected areas of cells adherent to monolayers presenting the FN9−10, FN10, and FN9m−10 proteins at each of the densities used above (Figure 7B). For each of the three proteins, we observed a substantial increase in average cell area as the density was increased from 0.001 to 0.01%. For monolayers presenting the FN9−10 and FN9m−10 fragments at 0.01% density, the projected areas averaged 1027 and 1002 μm^2, respectively, which were significantly higher than the average area of 805 μm^2 observed with the monolayer presenting the FN10 domain. For monolayers presenting the proteins at a density of 0.05%, the average area on FN10 increased to 910 μm^2 but was still significantly lower than the average spread areas for cells on FN9−10 and FN9m−10. It was only at a density of 0.1% that the projected areas of cells on all three substrates were comparable, at a value of approximately 1060 μm^2. These results indicate a modest role for the 9th domain, but not the PHSRN motif, in promoting cell spreading within only a narrow range of density.

PHSRN and RGD Competitively Inhibit Cell Attachment to Surfaces Presenting FN10. Given the previous experiments where the presence of PHSRN was shown to have a modest effect on cell attachment at low densities of protein but no effect on cell spreading, we performed additional adhesion experiments in the presence of soluble peptide inhibitors to determine any

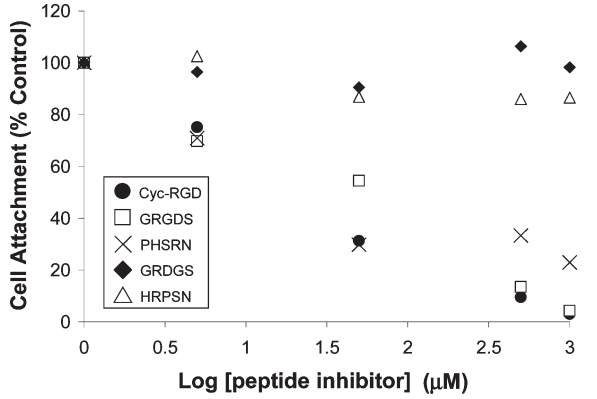

Figure 8. Inhibition of BHK cell attachment with soluble peptides to surfaces presenting FN10. Suspended cells were treated with cyclic-RGDfC, GRGDS, PHSRN, GRDGS, and HRPSN peptides at concentrations ranging from 5 μM to 1 mM and then allowed to attach to the FN10 surfaces at densities of 0.005% (RGD) or 0.001% (PHSRN). The number of cells that attached to the monolayers is shown for each concentration of inhibitor relative to the control surface that included no inhibitor. Each data point represents the average of three independent experiments with error bars omitted for clarity.

competition between the two ligands. We have previously reported that soluble PHSRN and RGD peptides competitively inhibited cell adhesion to monolayer surfaces presenting either peptide, although PHSRN was unable to fully prevent adhesion to RGD substrates due to its weaker affinity for the integrin.[32] Here, we performed similar inhibition experiments to determine whether both PHSRN and RGD peptides could block cell adhesion to FN10-presenting monolayers (Figure 8). We reduced the density of FN10 on the surface since monovalent ligands are poor inhibitors for polyvalent cell attachment.[62] We used substrate densities of 0.005% for experiments with cyclic-RGDfC, GRGDS, as well as the scrambled GRDGS, but reduced the density further to 0.001% with the PHSRN and HRPSN inhibitors because of the decreased ligand affinity. Also, as shown in the previous experiments, this range of density is where the presence of PHSRN had a modest synergistic effect on cell attachment. As expected, we found that both RGD peptides completely inhibited cell adhesion to FN10 with concentrations above 500 μM. We also found that cell adhesion was inhibited in the presence of PHSRN to 20−30% of the control at concentrations above 50 μM. Despite the incomplete inhibition due to its weaker affinity, this data shows that the peptide PHSRN is capable of blocking cell adhesion to FN10, thereby corroborating the competitive binding mechanism for the PHSRN and RGD ligands. If PHSRN and RGD were bound with a two-point binding mechanism, the presence of soluble PHSRN peptide would not be able to prevent the integrin cell receptor from binding to the immobilized FN10 domain containing the RGD motif. Additionally, the lack of inhibition shown with the scrambled GRDGS and HRPSN peptides confirms that the interaction is specific for the peptide sequences. Similar experiments were performed using FN9 substrates, but the low protein density and short adhesion time prevented sufficient cell adhesion to get an accurate inhibition plot.

Discussion

PHSRN and RGD Act Independently as Integrin Ligands for Cell Adhesion. By comparing cell adhesion and spreading on substrates presenting six distinct FN fragments that include the RGD and PHSRN motifs in active and inactive forms, we find that both ligands can independently mediate adhesion. Cells attach with comparable efficiency to monolayers presenting FN9−10, FN9, FN10, FN9−10m (mutated RGD site), and FN9m−10 (mutated PHSRN site), but fail to attach to a monolayer presenting the double mutant FN9m−10m. This finding that cells are able to adhere to substrates presenting only the PHSRN motif is consistent with recent studies,[32−34] though in conflict with several previous reports that find that PHSRN is unable to mediate cell adhesion itself,[21,22,24] and we address this discrepancy below. However, we find that significant cell spreading is dependent on substrates presenting an active RGD motif, and only for these substrates did cells display abundant FAs and organized actin cytoskeletons as shown through immunostaining. Additionally, we show that soluble RGD and PHSRN ligands are each capable of blocking cell adhesion to substrates presenting the FN10 domain, which adds further support that both bind competitively to the cell integrin receptors.

Unlike several studies that have demonstrated an apparent synergy between the RGD and PHSRN peptide motifs,[21,22,40,42] we find that cells attach with similar efficiency to monolayers presenting FN10 (or the analogous FN9m−10) and FN9−10. Hence, with one exception addressed below, we find that the presence of the PHSRN motif in the FN9 domain has little effect on increasing the efficiency of cell adhesion or spreading when it is present together with the RGD motif in the FN10 domain. We rule out a lack of synergy due to inaccessibility of the ligand—due, for example, to the orientation or density of the protein construct on the monolayer—because monolayers presenting either FN9m−10 or FN9−10m support cell adhesion, showing that both ligands, when present alone, interact with integrin receptors. We also note another report that suggests an additional synergistic area in FN9 could be responsible for enhanced cell attachment and spreading.[63] If this were the case, we would expect to see similar levels of cell attachment and spreading for FN9−10 and FN9m−10, but a distinct difference in cell area on FN10 since the entire FN9 domain is lacking. We observe this to a very modest extent, but only over a narrow range of lower densities. Taken together, our results point toward a different model for adhesion, one where the two peptides do not bind synergistically, but rather have independent roles in attachment and spreading and do not bind simultaneously to a single receptor. In an earlier report that used monolayers to present short peptide ligands for studies of cell adhesion, we found that both RGD and PHSRN mediated adhesion, though the latter with substantially lower affinity.[32] We also found that the addition of either peptide to the medium could inhibit cell attachment to either peptide substrate; that is, the two peptides bound competitively and not synergistically to the receptor. The current findings with model substrates that present protein domains—in place of the simplified peptide motifs—are consistent with this earlier study.

The predominant view holds that the PHSRN peptide is a synergy ligand and is not capable of mediating adhesion on its own but acts to enhance cell attachment and spreading when presented with RGD. To explain the mechanism of a synergistic activity, Obara and Yoshizato hypothesized that the PHSRN and RGD peptides bind to separate sites of a single integrin and while the former has insufficient affinity to mediate adhesion, when presented together with RGD, this two-point engagement displays a higher avidity for the receptor.[23] This model is consistent

(62) Mammen, M.; Choi, S. K.; Whitesides, G. M. *Angew. Chem., Int. Ed. Engl.* **1998**, *37*, 2755–2794.

(63) Redick, S. D.; Settles, D. L.; Briscoe, G.; Erickson, H. P. *J. Cell Biol.* **2000**, *149*, 521–527.

with the crystal structure of the 7th to 10th type III domains of FN that shows the two peptides reside on the same face of the protein and are separated by a distance that is suitable for interaction with a single integrin.[25] However, this model lacks conclusive support. On the basis of the residual density maps from an electron microscopy study, Arnaout suggested that FN9 is capable of binding to the αV integrin subunit while FN10 binds to β3,[64] a finding that is consistent with the individual crystal structures of the integrin αVβ3[26] and FN7−10 domains.[25] Yet these EM structures and model also propose that the integrin receptor remains in its bent state when bound to FN7−10, a hypothesis that has been contested and recently shown to be unlikely.[65] Using solution X-ray scattering, Mould and co-workers report structural data for α5β1 bound to FN6−10 at a resolution of 10 Å and also claim that the PHSRN and RGD sites have direct interaction with the α and β subunits of the integrin, respectively.[66]

However, Takagi and co-workers reported EM structures of α5β1 and FN7−10 with both native and mutated synergy regions and failed to find evidence for a direct contact between the integrin and synergy site.[67] In addition, kinetic data for the interaction of these two proteins shows that a single mutation of the arginine residue (to alanine) in the synergy region results in a 5-fold reduction on the association rate of the complex. Further mutations decrease the association rate another 20-fold, but the effect on the dissociation rate is only affected 2-fold. This strong influence over the association rate indicates that the synergy region may enhance the probability that the proteins form a complex following the initial integrin−FN encounter, and the lack of an effect on the dissociation rate signifies no major role in the stability of the protein−protein interaction. Takagi further explains these results and questions the relevancy of the two-site docking model in a later report.[45] Overall, these findings are consistent with our results that the PHSRN sequence does not assist RGD in cell spreading but that it can increase the efficiency of cell attachment when the ligands are present at certain densities. Along with our inhibition studies which confirm the two peptide ligands are competing for the same receptor binding site, we suggest that the presence of the PHSRN site increases the probability of initial adhesion by acting as an additional, weaker ligand to engage the cell integrins, but is eventually replaced by the stronger RGD ligand since it binds integrins with higher affinity.

A high-resolution structure of the α5β1 integrin in complex with FN has not yet been reported, but would serve an important role in distinguishing between the current models for the interaction of PHSRN and the receptor. In an analogous system, structures were recently reported at 2.4−2.8 Å resolution for the αIIbβ3 integrin bound to the γC and the RGD peptide ligands from fibrinogen.[68] These structures effectively resolved the controversy over whether γC and RGD compete for the same αIIbβ3 integrin adhesion site or bind to distinct sites. The structures show the lysine of the γC sequence bound in the same integrin pocket as the arginine residue of the RGD sequence, as well as the penultimate aspartic acid residue of the γC sequence bound to the metal ion-dependent adhesion site (MIDAS) as with the aspartic acid residue of RGD peptide. For the present question of the binding of α5β1 with PHSRN and RGD, inhibition studies here and in a previous report have shown that both PHSRN and RGD are capable of competitively binding to this integrin to block cell adhesion to substrates presenting either peptide.[32] Another study similarly showed that both RGD and a PHSRN-containing peptide could inhibit the interaction between the αIIbβ3 integrin and FN.[20] These reports, taken together with the adhesion data presented in this current study, support a model where PHSRN and RGD competitively bind to the same site in the integrin receptor to mediate cell adhesion.

The Role of Density in the Activity of PHSRN. While our initial experiments revealed no dependence on the PHSRN motif in the adhesion of cells to the RGD motif, and therefore were inconsistent with several earlier studies showing a synergistic effect, we questioned whether the density of the immobilized protein in our study was sufficiently high that the RGD ligand was present in an amount that far exceeded the number of integrin receptors presented on the cell surface. In this limit, the addition of an equal number of low affinity PHSRN ligands might be expected to have little effect on adhesion. Studies have shown that a typical fibroblast cell has about 500 000 integrin receptors on its surface,[69,70] which, given the average spread cell area of 1000 μm^2 observed in this study, corresponds to about 500 integrins/μm^2. This implies that a substrate having immobilized ligand at the same density (500 ligands/μm^2) would potentially be sufficient to engage each integrin on the cell surface. Previous SAM radiolabeling experiments established that monolayers with 1% density of ligand corresponded to nearly 40 000 ligands/μm^2,[43] which is more than enough ligand to engage each of the integrin receptors with the higher affinity RGD peptide.

Typical substrates for adhesion studies are formed by protein adsorption, and the ligand densities on these surfaces are known to vary widely. Previous studies reporting a synergy effect used substrates that were prepared by adsorbing proteins from solutions at concentrations ranging from 5 to 200 μg/mL.[21,22,71] It can be difficult to estimate the resulting density of *active* protein, but several studies have used radiolabeled matrix proteins at these concentrations and determined that the *total* densities of adsorbed molecules typically range from 30 to 2000 fmol/cm^2 (or about 200−12 000 ligands/μm^2).[39,72−74] However, this method does not identify what fraction of protein was present in an orientation and conformation that allows for interaction with an integrin receptor. Even ELISA cannot accurately predict the activity of an adsorbed ligand since the antibodies typically do not bind the same as the cell receptor. Additionally, because these substrates are not resistant to further protein adsorption, the surface density of ligand can change throughout an experiment.

Massia and Hubbell performed experiments with protein-resistant glass surfaces presenting radiolabeled RGD peptides and were able to prepare substrates with densities ranging from 0.001 to 12 000 fmol/cm^2.[39,75] They found that human foreskin fibroblast (HFF) cells could adhere and modestly spread on substrates having RGD present at densities as low as 1 fmol/cm^2, although organized FA and cytoskeletal structure required

(64) Adair, B. D.; Xiong, J. P.; Maddock, C.; Goodman, S. L.; Arnaout, M. A.; Yeager, M. *J. Cell Biol.* **2005**, *168*, 1109–1118.
(65) Zhu, J.; Boylan, B.; Luo, B. H.; Newman, P. J.; Springer, T. A. *J. Biol. Chem.* **2007**, *282*, 11914–11920.
(66) Mould, A. P.; Symonds, E. J.; Buckley, P. A.; Grossmann, J. G.; McEwan, P. A.; Barton, S. J.; Askari, J. A.; Craig, S. E.; Bella, J.; Humphries, M. J. *J. Biol. Chem.* **2003**, *278*, 39993–39999.
(67) Takagi, J.; Strokovich, K.; Springer, T. A.; Walz, T. *EMBO J.* **2003**, *22*, 4607–4615.
(68) Springer, T. A.; Zhu, J.; Xiao, T. *J. Cell Biol.* **2008**, *182*, 791–800.
(69) Neff, N. T.; Lowrey, C.; Decker, C.; Tovar, A.; Damsky, C.; Buck, C.; Horwitz, A. F. *J. Cell Biol.* **1982**, *95*, 654–666.
(70) Wiseman, P. W.; Brown, C. M.; Webb, D. J.; Hebert, B.; Johnson, N. L.; Squier, J. A.; Ellisman, M. H.; Horwitz, A. F. *J. Cell Sci.* **2004**, *117*, 5521–5534.
(71) Garcia, A. J.; Schwarzbauer, J. E.; Boettiger, D. *Biochemistry* **2002**, *41*, 9063–9069.
(72) Humphries, M. J.; Akiyama, S. K.; Komoriya, A.; Olden, K.; Yamada, K. M. *J. Cell Biol.* **1986**, *103*, 2637–2647.
(73) Singer, I. I.; Kawka, D. W.; Scott, S.; Mumford, R. A.; Lark, M. W. *J. Cell Biol.* **1987**, *104*, 573–584.
(74) Danilov, Y. N.; Juliano, R. L. *Exp. Cell Res.* **1989**, *182*, 186–196.
(75) Massia, S. P.; Hubbell, J. A. *Anal. Biochem.* **1990**, *187*, 292–301.

densities of at least 10 fmol/cm^2.[39] Together with the rationale presented above, this result implies the engagement of approximately 5−10% of the integrin receptors is sufficient to mediate cell adhesion and spreading.

In the work reported here, we used SAM substrates to present adhesive ligands at densities ranging from 0.00001 to 1%. Although the ratio of alkanethiols in solution does not strictly match the ratio of the alkanethiolates in the monolayer, our experience and other reports[76−78] suggest that the two ratios are similar in those cases where one oligo(ethylene glycol)-terminated alkanethiolate is present at low density relative to a second oligo(ethylene glycol)-terminated alkanethiolate. We note, however, that we have not independently verified the densities of the peptides in the monolayer substrates. Additionally, a previous study using radiolabeled peptides determined that monolayers with peptide densities of 0.1−1% corresponded to 700−7000 fmol/cm^2,[43] so we feel confident that these density values are reasonable. We found that cell adhesion on FN9−10 surfaces required a minimum density of 0.0001% (about 0.7 fmol/cm^2), a value that generally agrees with the 1 fmol/cm^2 density that Hubbell and Massia determined was required for minimum adhesion. However, adhesion to FN10 and FN9m−10 required a minimum density of 0.001% or about 7 fmol/cm^2. In addition, for substrates with protein densities of 0.0001% and 0.001%, there was a significantly higher level of cell attachment to FN9−10 as compared to FN10 or FN9m−10. Hence, at limiting densities of peptide, we find that the presence of the PHSRN motif with the RGD motif increases the probability that cells will attach to the substrates compared to those that otherwise present only RGD. We do not believe that both the PHSRN and RGD motifs in the same protein construct can simultaneously engage distinct integrin receptors, but rather that the increased density of adhesive ligands increases the probability that a critical number of integrin receptors bind to immobilized ligands during the time a suspended cell encounters the substrate. Supporting this explanation, Springer has presented kinetic data for the $\alpha5\beta1$ integrin with a FN7−10 protein with several synergy mutations that shows a 5- or 26-fold reduction of the association rate of the complex when compared to a FN protein containing the native synergy sequence.[67] We speculate that this effect is directly linked to the density of immobilized ligand and that the presence of a sufficient density of RGD renders any PHSRN ligand unnecessary.

Additionally, we did not observe a similar synergistic effect on cell spreading. Instead, we found that the projected areas of adherent cells significantly increased for all protein substrates between densities of 7−70 fmol/cm^2. This threshold density of ligand is similar to the densities reported by Massia and Hubbell, where cell spreading was observed above a density of 1 fmol/cm^2.[39] We do, however, find a slightly sensitive dependence of spreading on density for surfaces that present FN10, as compared to surfaces that present both the 9th and 10th domains (FN9−10 and FN9m−10). This result, which does not depend on the activity of the PHSRN motif, suggests the potential for additional sites or weak interactions other than with PHSRN to synergistically increase cell spreading, as has been suggested in another report.[63] Overall, our studies show that PHSRN is capable of mediating cell attachment without the presence of RGD and can also increase cell attachment synergistically with RGD when ligand density is low, but PHSRN has insufficient affinity to support cell spreading and cytoskeletal organization on its own.

SAMs are Effective Model Substrates for Cell Adhesion. The role of PHSRN in cell adhesion was first recognized some 15 years ago and was followed by the proposal of a synergy binding model—that is, a model wherein the RGD and PHSRN ligands interact cooperatively with independent sites on an integrin receptor—although other data has accumulated that it is consistent with a model wherein the two peptides are mutually exclusive ligands for the receptor. Despite substantial work over the past decade, the question remains open. We suggest that this ambiguity stems from the limitations that are inherent to the experimental tools used in studies of cell adhesion. For experiments that compare cell adhesion and spreading to substrates prepared by adsorbing protein to a material, it is impractical to rule out effects due to changes in the conformations or orientations of the adsorbed protein. Recent work by Mardon and coworkers maintains that the synergistic activity of the 9th domain is dependent on its structural stability, which is presumably related to the tendency of proteins to denature upon adsorption.[30,79] We also note an early study in this field that failed to observe cell adhesion to a surface coated with a protein FN fragment having both the PHSRN and RGD motifs, a result that can clearly be attributed to the ambiguities inherent to protein adsorption.[16] Other studies have used electron microscopy to visualize integrin−FN complexes, but these approaches have resulted in compelling reports both in support of and against the synergy model.[26,67] Here again, it is difficult to rule out artifacts that stem from the interaction of the protein complex with the electron microscopy grid and that can perturb the equilibrium structure of the complex.

We believe that the model substrates used in this work avoid many of these limitations and provide a functional context to compare cell adhesion to substrates presenting fragments of the FN protein. By allowing control over the density and orientation of protein and by reducing artifacts associated with nonspecific interaction of proteins with materials, the monolayers are an effective model for identifying structure−function relationships of the ECM. The results in this work, together with a previous report that used peptide-modified monolayers, are consistent with a model wherein the RGD and PHSRN motifs bind competitively to an integrin receptor, and where the former has a higher affinity and can support cell spreading and cytoskeletal organization. For substrates that present low densities of the protein, the presence of the lower affinity PHRSN motif has an effect in promoting attachment. This approach using monolayers as models of the ECM should be important for addressing a broader range of questions in the biology of cell adhesion to the ECM.

Acknowledgment. We thank Dr. Harold Erickson for providing the FNIII7-10(pET11b) plasmid used for this work. We also thank Jacob Basak for synthesizing the phosphonate-thiol ligand used in these experiments. This work was supported by the NIH (R01GM068587) and a MURI grant from the Army Research Office (W911NF-04-1-071).

Supporting Information Available: Primers and experimental details regarding the construction of the cutinase−fibronectin domain fusion proteins as well as cell adhesion data showing protein density dependence. This material is available free of charge via the Internet at http://pubs.acs.org.

(76) Folkers, J. P.; Laibinis, P. E.; Whitesides, G. M.; Deutch, J. *J. Phys. Chem.* **1994**, *98*, 563–571.
(77) Mrksich, M.; Grunwell, J. R.; Whitesides, G. M. *J. Am. Chem. Soc.* **1995**, *117*, 12009–12010.
(78) Roberts, C.; Chen, C. S.; Mrksich, M.; Martichonok, V.; Ingber, D. E.; Whitesides, G. M. *J. Am. Chem. Soc.* **1998**, *120*, 6548–6555.
(79) Altroff, H.; Choulier, L.; Mardon, H. J. *J. Biol. Chem.* **2003**, *278*, 491–497.